# Heavy-hole scattering by confined nonpolar optical phonons in a single $Si_{1-x}Ge_x$/Si quantum well

Gregory Sun
*Engineering Program, University of Massachusetts at Boston, Boston, Massachusetts 02125*

Lionel Friedman
*Rome Laboratory/EROC, Hanscom Air Force Base, Bedford, Massachusetts 01731*
(Received 14 July 1995)

Intrasubband and intersubband scattering rates of heavy holes are obtained due to confined nonpolar optical phonons in a $Si_{1-x}Ge_x$ quantum well with Si barriers. Guided and interface Ge-Si and Ge-Ge modes and unconfined Si-Si modes are considered. A continuum model is used for the two components of the ionic displacement of confined vibrations: the uncoupled *s*-polarized TO mode and the hybrid of the LO and *p*-polarized TO modes. The guided mode is obtained using the model of a quantum well with infinitely rigid barriers and the interface mode is derived from the hydrodynamic boundary conditions. While the total intersubband scattering rates are reduced as a result of confinement, the opposite is found for the intrasubband scattering. Depending on the well width and Ge content, the intersubband scattering rates are reduced by a factor of 2–4 with respect to their values for no confinement. Thus one would expect comparable enhancement in the intersubband lifetimes crucial to the population inversion in a $Si_{1-x}Ge_x$/Si intersubband laser.

## I. INTRODUCTION

The possibility of lasing due to intersubband transitions in quantum-well (QW) structures is crucially dependent on the lifetimes of the involved subbands. In an earlier Letter[1] lifetimes were calculated for a $Si_{1-x}Ge_x$/Si multiple-quantum-well (MQW) structure due to acoustic- and nonpolar optical-phonon scattering. It was pointed out that, because of the absence of polar optical scattering for silicon-based systems, the lifetimes and their differences are consistently an order of magnitude larger than for the GaAs/$Al_xGa_{1-x}As$ system and do not show the marked decrease when the intersubband energy exceeds the optical-phonon energy. For this case, the scattering was calculated for propagating phonons corresponding to the average composition, assuming no confinement. As pointed out in that paper, it is expected that this treatment of phonon scattering leads to an overestimate of the intersubband transition rates and therefore provides a conservative approach in determining the subband lifetimes. In order to more accurately determine the subband lifetimes, it is necessary to take into account confinement effects on optical phonons in heterostructures. In a $Si_{1-x}Ge_x$/Si QW structure, one can expect Si-Si, Ge-Si, and Ge-Ge optical modes in the alloy.[2] The Ge-Si and Ge-Ge modes tend to be confined by the Si barriers, as has been seen in Raman scattering experiments.[3] The phonon confinement gives rise to guided and interface modes, which will scatter the carrier less for intersubband transitions, thus resulting in revised subband lifetimes. This is due to the discrete spectrum of the guided modes and the weak intersubband scattering of interface modes. However, the intrasubband scattering process tends to be enhanced due to confinement.

There has been a great deal of effort in dealing with the issue of phonon confinement in heterostructures.[2–21] Most of published literature has focused on confined polar optical phonons, because a large body of the heterostructures is constructed from polar semiconductor materials. Recently, the demonstration of an infrared intersubband transition laser in the $In_yGa_{1-y}As/Al_xGa_{1-x}As$ material system[22] has renewed interest in investigating the possibility of constructing lasers within the Ge/Si material system, which eventually would allow monolithic integration of optical components with advanced Si microelectronics.[23]

A self-consistent continuum theory of confined nonpolar optical phonons has been developed for an infinite plate with free boundary conditions.[4] In the present paper, we extend that continuum theory to examine the confined nonpolar optical phonons of Ge-Si and Ge-Ge vibration modes with proper mechanical boundary conditions in a $Si_{1-x}Ge_x$/Si QW. Furthermore, we use these results to estimate the heavy-hole scattering rates by the nonpolar optical phonons. To the best of our knowledge, there has not been any work in estimating the scattering rates due to the nonpolar optical phonons in $Si_{1-x}Ge_x$/Si heterostructures taking into account phonon confinement.

The three different vibration modes, namely, Si-Si, Ge-Si, and Ge-Ge, are considered separately and are given proper weights in heavy-hole scattering calculation. The Si-Si mode propagates freely throughout the structure, while the Ge-Si and Ge-Ge modes are confined by the barriers, resulting in guided and interface modes. Approximations made in the course of the calculations for the guided and interface modes will be discussed. We will examine both intrasubband and intersubband scattering processes. We will also compare these results with those assuming no confinement. We will show that indeed the latter assumption overestimates the scattering rates for intersubband transitions, but tends to underestimate the intrasubband process. The difference is largely attributed to the heavy-hole interaction with interface modes, which can be neglected for the intersubband process, but contributes significantly to the intrasubband process. The scattering rates due to various scattering modes will be investigated as a function of the well width and as a function of the alloy composition of the well.

 

## II. PHONON CONFINEMENT

Phonon confinement occurs due to the lack of overlap of the bulk frequency dispersions in the adjacent heterostructure materials. Thus in a Si/Ge/Si short period superlattice, the higher-frequency optical modes of Si correspond to a frequency gap in the Ge layer and are therefore confined. The Ge modes in the Ge layers are strictly resonant with the Si acoustic modes and are ''quasiconfined,'' but the displacement pattern is similar to that of a true confined mode and indeed the Raman intensities are comparable.[2] The Raman spectrum has revealed that there exist Ge-Ge, Ge-Si, and Si-Si vibration modes in the $Si_{1-x}Ge_x$ alloy layer.[3] The Ge-Ge vibrations have phonon energy of 37.4 meV and the Ge-Si vibrations of 50.8 meV. These two modes of the $Si_{1-x}Ge_x$ well are confined by the Si-Si modes of the barrier (phonon energy 64.3 meV); however, the Si-Si optical modes of the well are unconfined, as are the Si-Si optical modes of the barrier.

One of the simplest conceptual model is to treat the QW system with infinitely rigid barrier. The boundary condition to be satisfied is the vanishing of the ionic displacement of all confined vibration modes. This is an assumption of strict confinement, yielding guided modes of the confined phonons. This assumption needs to be partially relaxed in order to admit interface modes. As pointed out in the continuum theory,[4] the ionic displacement of confined vibrations has two components: one is the hybrid of the LO and $p$-polarized TO ($p$-TO) modes and the other is the uncoupled $s$-polarized TO ($s$-TO) mode. These modes are defined as follows: if we consider a $(x,z)$ plane containing the normal to the layers and the phonon wave vector $\mathbf{Q}$, then

$$\mathbf{Q}=q_x\hat{\mathbf{e}}_x+q_z\hat{\mathbf{e}}_z, \tag{1}$$

where $\hat{\mathbf{e}}_x$ and $\hat{\mathbf{e}}_z$ are unit vectors. The $p$-TO mode has its displacements normal to $\mathbf{Q}$ and in the $(x,z)$ plane, while the $s$-TO displacements are normal to $\mathbf{Q}$ and perpendicular to the $(x,z)$ plane ($\| \hat{e}_y$). A description of the $s$-TO mode is

$$u_y=e^{iq_xx}(Ae^{iq_zz}+Be^{-iq_zz}), \tag{2}$$

while the hybrid of the LO and $p$-TO modes is given by[4]

$$\begin{aligned} u_x&=e^{iq_xx}[q_x(Ce^{iq_Lz}+De^{-iq_Lz})+q_T(Ee^{iq_Tz}+Fe^{-iq_Tz})],\\ u_z&=e^{iq_xx}[q_L(Ce^{iq_Lz}-De^{-iq_Lz})-q_x(Ee^{iq_Tz}-Fe^{-iq_Tz})]. \end{aligned} \tag{3}$$

The $z$ components of the LO and TO wave vector have been distinguished by $q_L$ and $q_T$, respectively.

The above choice for the ionic displacement guarantees that

$$\nabla\times\mathbf{u}_L=0, \quad \nabla\cdot\mathbf{u}_T=0, \tag{4}$$

which hold for isotropic materials (assumed here), allowing $\mathbf{u}$ to be decomposed into LO and TO components

$$\mathbf{u}=\mathbf{u}_L+\mathbf{u}_T. \tag{5}$$

Since the LO and TO modes must have the same frequency to be effectively coupled, they have to satisfy, according to the bulk LO and TO dispersions,

$$\omega^2=\omega_0^2-\beta_L^2(q_x^2+q_L^2)=\omega_0^2-\beta_T^2(q_x^2+q_T^2), \tag{6}$$

where $\beta_L$ and $\beta_T$ are the velocities of LO and TO dispersions, respectively.

### A. Guided modes

In the case of strict confinement, the boundary condition of course is that the displacements $\mathbf{u}$ vanish at the boundaries $z=(0,L)$. For the $s$-TO mode, this leads to

$$u_y=Ae^{iq_xx}\sin(q_zz) \quad \text{with} \quad q_z=\frac{n\pi}{L}, \tag{7}$$

where $n=1,2,\ldots$. This mode does not mix with other modes, nor does it give rise to the interface mode discussed later. The $s$-TO mode pattern for $q_z=\pi/L$ is shown in Fig. 1(a) with the well width $L=40$ Å.

For the coupled LO and $p$-TO modes, applying the boundary conditions of $u_x=0$ and $u_z=0$ at $z=(0,L)$ to Eq. (3) leads to a system of four constant-coefficient linear equations for $C,D,E$, and $F$. The vanishing of the determinant of the $4\times4$ constant coefficient matrix gives rise to the relation

$$\begin{aligned} &(q_Tq_L+q_x^2)^2\sin(q_TL)\sin(q_LL)\\ &\quad=2q_Tq_Lq_x^2[\cos(q_T-q_L)L-1]. \end{aligned} \tag{8}$$

Equation (8) leads to solutions of guided modes consisting of coupled phase-matched LO and TO modes with wave vectors

$$q_L=\frac{n_L\pi}{L}, \quad q_T=\frac{n_T\pi}{L}, \tag{9}$$

where $n_L=1,2,\ldots$, $n_T=3,4,\ldots$, and $n_T-n_L=2,4,6,\ldots$. This choice of quantum numbers is due to the constraint Eq. (6) since $\beta_T<\beta_L$.

Two sets of guided mode solutions emerge and they are given in either sine or cosine form referring to the $z$ component of the ionic displacement. The ''sine'' solution is

$$\begin{aligned} u_x&=2Ce^{iq_xx}q_x[\cos(q_Lz)-\cos(q_Tz)],\\ u_z&=2iCe^{iq_xx}\left[q_L\sin(q_Lz)+\frac{q_x^2}{q_T}\sin(q_Tz)\right], \end{aligned} \tag{10}$$

and the ''cosine'' solution

$$\begin{aligned} u_x&=2iCe^{iq_xx}\left[q_x\sin(q_Lz)+\frac{q_Lq_T}{q_x}\sin(q_Tz)\right],\\ u_z&=2Ce^{iq_xx}q_L[\cos(q_Lz)-\cos(q_Tz)]. \end{aligned} \tag{11}$$

The hybrid patterns of the $p$-TO and LO modes with $q_L=\pi/L$ and $q_T=3\pi/L$ are shown in Figs. 1(b) and 1(c) for the sine and cosine solutions, respectively, with the well width $L=40$ Å.

It is worthwhile to point out the similarities between the allowed values of $q_z$, $q_L$, $q_T$, and $q_x$ for the guided modes in

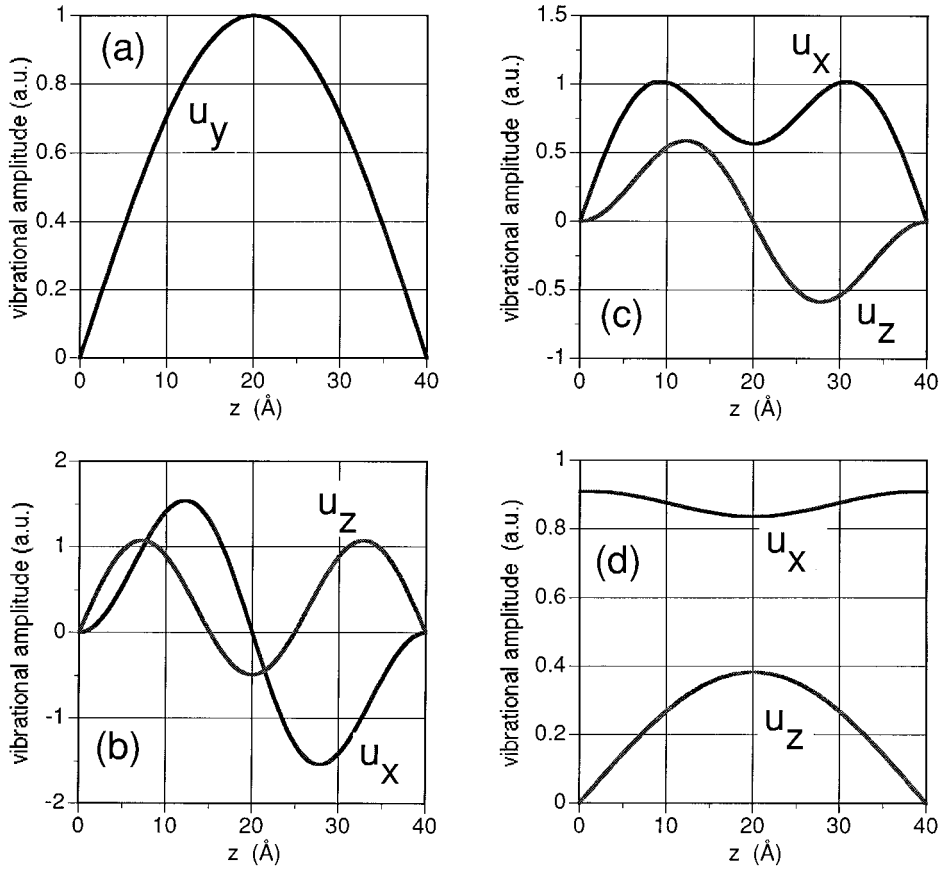


FIG. 1. Vibration patterns for (a) the guided $s$-TO mode, (b) the ''sine'' solution, (c) the ''cosine'' solution of the guided $p$-TO and LO modes, and (d) the coupled $p$-TO and LO interface mode for the well width of 40 Å.

the case of infinitely rigid barriers assumed here and that of an infinite plate with free boundary conditions.[4] But the displacement patterns differ dramatically between the two situations.

As pointed out by Mori and Ando,[13] Nash,[14] and Register,[15] a sum rule can be derived for polar optical scattering relating the form factors of the confined modes to that of the ''bulk'' modes. Such a sum rule, as pointed out by Nash,[14] arises from the completeness and orthogonality of the vibration sets. As derived, this applies to polar optical scattering accompanied by a macroscopic electrical potential. As is well known, the latter removes the degeneracy of the zone center optical phonons and the carrier interacts only with the LO mode. However, for the nonpolar optical phonons of interest in the present work, both TO and LO modes interact with the carrier. As discussed earlier, the $s$-TO mode does not mix with the other modes and can be described in terms of an orthogonal and complete set of functions given by Eq. (7). However, the $p$-TO and LO modes are coupled as given by Eqs. (10) and (11), with the constraint given by Eq. (6) that the frequencies be equal, taking account of the different frequency dispersions. The LO and $p$-TO modes cannot be treated independently because, having chosen their forms to satisfy Eq. (4), the vanishing boundary conditions at $z=0$ and $L$ cannot be satisfied for $\mathbf{u}_L$ and $\mathbf{u}_T$ independently. As a consequence of the coupling, in satisfying the boundary conditions for the guided modes, not all values of wave vectors $(q_x, q_L, q_T)$ are allowed and so the set is not complete. Specifically, the allowed values of $(q_L, q_T)$ require that $q_x$ be discrete, not continuous, and be given by

$$q_x^2 = \left(\frac{\pi}{L}\right)^2 \frac{\beta_T^2 n_T^2 - \beta_L^2 n_L^2}{\beta_L^2 - \beta_T^2}, \tag{12}$$

where $n_L$ and $n_T$ have been defined in Eq. (9). Further, two modes that differ in only one of $(q_L, q_T)$ are not orthogonal. In summary, in comparison with the guided modes for polar optical phonons, even though the guided modes constitute a complete orthogonal set for the $s$-TO modes in the $y$ direction, the linear combination of $p$-TO and LO modes in the $(x,z)$ plane are neither complete nor orthogonal. Hence a sum rule cannot be applied to the current basis set for nonpolar optical phonons.

### B. Interface modes

The assumption of strict confinement that the vibration amplitudes are zero at the interfaces rules out the possibility of interface modes. In general, such modes exist and are of increasing importance in carrier scattering intrasubband transitions in comparison with guided modes. The assumption of strict confinement must therefore be relaxed to admit such modes. It is obvious that the amplitudes of interface modes at the boundaries should remain small in order to keep the assumption of strict confinement yielding the guided modes. In

fact, we need only to relax the vanishing assumption of the $x$ component of the displacement to admit interface modes while maintaining the zero boundary condition on the $z$ component. A similar boundary condition has been employed in treating the polar optical phonons for a single GaAs/AlAs QW.[10]

Applying the hydrodynamic boundary conditions[5] at the interfaces to the LO and TO modes independently and considering the fact that the optical-phonon frequency in the barrier region is greater than that in the well region, we obtain only a solution with an even $z$ component for the LO mode,

$$\mathbf{u}_L=\begin{cases} Ce^{iq_x x}(q_x\hat{\mathbf{c}}_x-q_{L2}\hat{\mathbf{e}}_z)e^{-iq_{L2}z}, & z<0 \\ Ce^{iq_x x}\left(\dfrac{\rho_1}{\rho_2}\right)^{1/2}\left(\dfrac{\eta_2}{\eta_1}\dfrac{\rho_2}{\rho_1}q_x\hat{\mathbf{e}}_x-q_{L2}\hat{\mathbf{e}}_z\right), & 0<z<L \\ -Ce^{iq_x x}(q_x\hat{\mathbf{e}}_{\mathbf{x}}+q_{L2}\hat{\mathbf{e}}_z)e^{iq_{L2}(z-L)}, & z>L, \end{cases} \tag{13}$$

where the subscripts 1 and 2 refer to well ($Si_{1-x}Ge_x$) and barrier (Si) regions, respectively, $\rho_i$ is the material density, and

$$\eta_i=\omega_i^2/\omega^2-1, \tag{14}$$

where $\omega_i$ is the $\Gamma$-point optical-phonon frequency in layer $i$ ($=1,2$). For both Ge-Si and Ge-Ge confined modes we have $\omega_2>\omega_1$. The LO wave vector in the well region $q_{L1}=0$ and that in the barrier region

$$q_{L2}^2=\frac{\omega_2^2-\omega_1^2}{\beta_2^2}+\left(\frac{\beta_1^2}{\beta_2^2}-1\right)q_x^2. \tag{15}$$

The LO mode solution is of two-dimensional bulk type with constant amplitudes in the well region propagating with wave vectors parallel to the interfaces.

Both odd and even solutions emerge for the TO mode, but the boundary condition that the $z$ component of $\mathbf{u}_L+\mathbf{u}_T$ vanishes at the interfaces admits only the even solution

$$\mathbf{u}_T=\begin{cases} De^{iq_x x}(q_{T2}\hat{\mathbf{e}}_x+q_x\hat{\mathbf{e}}_z)e^{-iq_{T2}z}, & z<0 \\ De^{iq_x x}\left(\dfrac{\rho_1}{\rho_2}\right)^{1/2}\dfrac{1}{\cos(q_{T1}L/2)}[-iq_{T1}\sin(q_{T1}(z-L/2))\hat{\mathbf{e}}_x+q_x\cos(q_{T1}(z-L/2))\hat{\mathbf{e}}_z], & 0<z<L \\ -De^{iq_x x}(q_{T2}\hat{\mathbf{e}}_x-q_x\hat{\mathbf{e}}_z)e^{iq_{T2}(z-L)}, & z>L, \end{cases} \tag{16}$$

where the wave vectors for the TO mode, according to Eq. (6),

$$\begin{aligned} q_{T1}^2&=\left(\frac{\beta_{L1}^2}{\beta_{T1}^2}-1\right)q_x^2 \quad \text{(well)}, \\ q_{T2}^2&=\left(\frac{\beta_{L2}^2}{\beta_{T2}^2}-1\right)q_x^2+\frac{\beta_{L2}^2}{\beta_{T2}^2}q_{L2}^2 \quad \text{(barrier)}. \end{aligned} \tag{17}$$

Combining Eqs. (13) and (16) and applying that the $z$ component of $\mathbf{u}_L+\mathbf{u}_T$ vanishes at the interfaces lead to $D=(q_{L2}/q_x)C$ and finally the interface mode is obtained

$$\mathbf{u}=\begin{cases} Ce^{iq_x x}\left[\left(q_x e^{-iq_{L2}z}+\dfrac{q_{L2}q_{T2}}{q_x}e^{-iq_{T2}z}\right)\hat{\mathbf{e}}_x+(-q_{L2}e^{-iq_{L2}z}+q_{L2}e^{-iq_{T2}z})\hat{\mathbf{e}}_z\right], & z<0 \\ Ce^{iq_x x}\left(\dfrac{\rho_1}{\rho_2}\right)^{1/2}\left\{\left[\dfrac{\eta_2}{\eta_1}\dfrac{\rho_2}{\rho_1}q_x-\dfrac{i}{\cos(q_{T1}L/2)}\dfrac{q_{L2}q_{T1}}{q_x}\sin(q_{T1}(z-L/2))\right]\hat{\mathbf{e}}_x+q_{L2}\left[\dfrac{\cos(q_{T1}(z-L/2))}{\cos(q_{T1}L/2)}-1\right]\hat{\mathbf{e}}_z\right\}, & 0<z<L \\ Ce^{iq_x x}\left\{\left[-q_x e^{iq_{L2}(z-L)}-\dfrac{q_{L2}q_{T2}}{q_x}e^{iq_{T2}(z-L)}\right]\hat{\mathbf{e}}_x+[-q_{L2}e^{iq_{L2}(z-L)}+q_{L2}e^{iq_{T2}(z-L)}]\hat{\mathbf{e}}_z\right\}, & z>L. \end{cases} \tag{18}$$

Figure 1(d) shows the pattern of an interface mode in the well region responsible for the scattering process from subband 2 to 1 by emitting a Ge-Si optical phonon, with $L=40$ Å. It can be seen from Fig. 1(d) that the $x$ component of the displacement is approximately constant within the well region and the $z$ component vanishes at both interfaces.

The above form of the interface mode derived from the hydrodynamic boundary conditions is different from that of the surface mode for the infinite free plate[4] and that for the interface mode for polar materials. The difference from the former case arises from the different boundary conditions since the free surface requires that the dilation stress perpendicular to the surface and the shear stress across the surface vanish. The difference from the latter is primarily due to the fact that the zone-center optical-phonon frequency in the barriers is greater than that in the well, which is contrary to the situation in GaAs/$Al_xGa_{1-x}$As material systems.

The dispersion of the bulk Si-Si mode has little overlap with that of the Ge-Si mode. The scattering process involves only long-wavelength in-plane wave vectors and the $z$ components of phonon wave vectors in the barriers, $q_{L2}$ and $q_{T2}$, are approximately the dimension of the Brillouin zone. This

is because the dispersion relations overlap only at large phonon wave vectors in the barrier region. Since $q_{L1}=0$ and $q_x \approx 0$, the interface mode frequency $\omega \approx \omega_1$, therefore, $\eta_2/\eta_1 \gg 1$. The major scattering contributions from the interface mode is from the displacement in the well region where the heavy holes are confined. The amplitude of the LO component is much greater than that of the TO component in Eq. (18) for $0<z<L$, since

$$\frac{\eta_2}{\eta_1}\frac{\rho_2}{\rho_1} \gg \frac{q_{L2}q_{T1}}{q_x^2}, \tag{19}$$

considering $q_{T1}$ also small. Therefore, the exact values of $q_{L2}$ and $q_{T2}$ are not crucial in determining the scattering rates because the TO mode contribution is at least two orders of magnitude less than the LO mode. The above displacement pattern Eq. (18) has been used in evaluating the interface mode scattering for the confined Ge-Si and Ge-Ge modes.

## III. HEAVY-HOLE SCATTERING RATES

The nonpolar optical-phonon interaction Hamiltonian involving a heavy hole is[24]

$$H=\frac{(M_1M_2)^{1/2}}{M_1+M_2}\mathbf{D}\cdot\mathbf{u}, \tag{20}$$

where $M_1$ and $M_2$ are the masses of the two atoms in the unit cell and $\mathbf{D}$ is the optical deformation potential. The normalization of the displacement amplitudes is carried out through the approach of equating the energy of the vibration mode with that of a simple harmonic oscillator[9] as

$$\chi^2=\frac{S}{\Omega}\int_0^L \mathbf{u}^*\cdot\mathbf{u}\, dz, \tag{21}$$

where $L$ is the well width, $S$ is the sample surface area [in the $(x,y)$ plane], $\Omega$ is the volume of the unit cell, and $\chi$ is the normal coordinator of the oscillator.

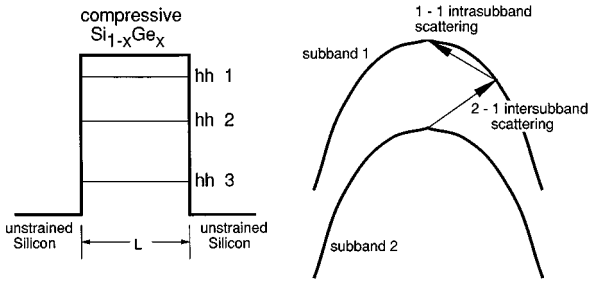


FIG. 2. Heavy-hole (hh) band structure and scattering processes.

The heavy-hole band offset is calculated taking into account the compressive strain in the $Si_{1-x}Ge_x$ well region.[25] The heavy-hole bands are decoupled from the light-hole and split-off bands at $\mathbf{k}=0$ and can be treated independently.[26] The heavy-hole energy levels and envelope wave functions are obtained by the finite square well model as shown in Fig. 2. The heavy-hole state can be characterized by $|\mathbf{k},n\rangle$ with the in-plane momentum $\mathbf{k}$ and subband index $n$. In the approximation of constant effective mass for heavy holes, the matrix element for the transition from state $|\mathbf{k},n\rangle$ to $|\mathbf{k}',n'\rangle$ due to nonpolar optical phonon scattering is

$$\langle \mathbf{k}',n'|H|\mathbf{k},n\rangle=\begin{cases}\left(\dfrac{\hbar[n(\omega_0)+\frac{1}{2}\mp\frac{1}{2}]}{2\rho_1\omega_0 SL\Delta_A(q_z)}\right)^{1/2}\delta_{\mathbf{k}'\pm\mathbf{q}_x,\mathbf{k}}D_y G^y_{nn'}(q_z) & (s\text{-TO})\\ \left(\dfrac{\hbar[n(\omega_0)+\frac{1}{2}\mp\frac{1}{2}]}{2\rho_1\omega_0 SL\Delta_C(q_L,q_T)}\right)^{1/2}\delta_{\mathbf{k}'\pm\mathbf{q}_x,\mathbf{k}}[D_x G^x_{nn'}(q_L,q_T)+D_z G^z_{nn'}(q_L,q_T)] & (\text{hybrid})\end{cases} \tag{22}$$

for the $s$-TO mode and the hybrid of the LO and $p$-TO mode, respectively. $n(\omega_0)$ is the number of optical phonons at thermal equilibrium and the upper and lower signs refer to phonon absorption and emission, respectively. The three components of the optical deformation potential $D_x$, $D_y$, and $D_z$ are assumed to be equal to $D_0=D/\sqrt{3}$ in the calculation, in view of the assumption of isotropy. The Kronecker delta indicates the in-plane $(x,y)$ momentum conservation. The normalization factors are given by

$$\Delta_A(q_z)=\frac{1}{L}\int_0^L u_y^* u_y dz \quad (s\text{-TO}),$$
$$\Delta_C(q_L,q_T)=\frac{1}{L}\int_0^L (u_x^* u_x+u_z^* u_z)dz \quad (\text{hybrid}). \tag{23}$$

The $G_{nn'}$ functions contain envelope wave functions $\psi_n$ and $\psi_n'$ from which interference effects can be obtained. Specifically,

$$G^y_{nn'}(q_z)=\int_0^L \psi_n\psi_{n'}u_y dz \tag{24}$$

for the $s$-TO mode and

$$G^x_{nn'}(q_L,q_T)=\int_0^L \psi_n\psi_{n'}u_x dz,$$
$$G^z_{nn'}(q_L,q_T)=\int_0^L \psi_n\psi_{n'}u_z dz \tag{25}$$

for the hybrid of LO and $p$-TO modes. It should be noted that, given the proper displacement expressions, Eq. (22) for the matrix element is valid for both the guided and interface modes discussed above.

Obviously, depending on the alloy composition in the well, the three modes (Si-Si, Ge-Si, and Ge-Ge) will have different interaction strengths with the carriers in the QW structure. Specifically, each interaction should be weaker

than that for the case where it is the only existing mode and therefore needs to be accounted for properly. A crude model to approximate the relative strength of each individual mode is to assign a weight in the calculation of the phonon scattering rate. If we assume bonds formed between Si-Si, Ge-Si, and Ge-Ge are purely random, then we can give the following weights according to the Ge content $x$ to each of the vibration modes in the $Si_{1-x}Ge_x$ well: $w_{Si}=(1-x)^2$ for the Si-Si mode, $w_{GeSi}=2x(1-x)$ for the Ge-Si mode, and $w_{Ge}=x^2$ for the Ge-Ge mode.

Applying the Fermi golden rule, we obtain the scattering rate due to the guided modes

$$W^j_{nn'}=\begin{cases}\dfrac{w_j m^*_{hh}[n(\omega_0)+\frac{1}{2}\mp\frac{1}{2}]D_0^2}{2\hbar^2\rho_1\omega_0 L}\displaystyle\sum_{q_z}\frac{|G^y_{nn'}|^2}{\Delta_A} & (s\text{-TO})\\ \dfrac{w_j m^*_{hh}[n(\omega_0)+\frac{1}{2}\mp\frac{1}{2}]D_0^2}{2\hbar^2\rho_1\omega_0 L}\displaystyle\sum_{q_L,q_T}\frac{|G^x_{nn'}+G^z_{nn'}|^2}{\Delta_C} & (\text{hybrid}),\end{cases} \tag{26}$$

where we have assumed that for the intersubband process ($n\neq n'$) the heavy holes are scattered from the bottom of their original subbands and for the intrasubband process ($n=n'$) the heavy holes have just enough kinetic energy (equal to the Si-Si optical-phonon energy) to emit an optical phonon to reach to the bottom of the same subband. $w_j$ (where $j$ denotes Ge-Si or Ge-Ge) is the weight assigned to a particular vibration mode and $m^*_{hh}$ is the heavy-hole effective mass.

For the $s$-TO guided mode, the summation in Eq. (26) is over all $q_z=n\pi/L$ limited by

$$q_z^2<\left(\frac{\pi}{a_j}\right)^2-q_x^2, \tag{27}$$

where $a_j$ is the lattice constant and $q_x$ is given by the constraint of the in-plane momentum conservation. For the hybrid guided mode, the summation is restricted to those combinations of $q_L=n_L\pi/L$ and $q_T=n_T\pi/L$, which, according to Eq. (6), yield discrete values of $q_x$ satisfying the in-plane momentum conservation. It should be pointed out that a unique final-state heavy-hole wave vector $\mathbf{k}'$ (initial $\mathbf{k}=\mathbf{0}$) will result if the phonon frequency dispersion is neglected, corresponding to a constant optical-phonon energy. Then the in-plane momentum conservation would be impossible since the discrete values of $q_x$ will not be able to exactly match the unique value of $\mathbf{k}'$. However, taking into account of the phonon dispersion, a region of heavy-hole wave vector $\mathbf{k}'$ will be obtained and the scattering process is permitted as long as $q_x$ lies in that region.

There is no $s$-TO interface mode and the scattering rate due to the hybrid interface mode can be given, similarly, by

$$W^j_{nn'}=\frac{w_j m^*_{hh}[n(\omega_0)+\frac{1}{2}\mp\frac{1}{2}]D_0^2}{2\hbar^2\rho_1\omega_0 L\Delta_C}|G^x_{nn'}+G^z_{nn'}|^2, \tag{28}$$

where $G^x_{nn'}$ and $G^z_{nn'}$ are functions of $q_{T1}$, $q_{L2}$, and $q_{T2}$ with $q_{L1}=0$. The determination of the phonon wave vectors in the well and barrier regions has been discussed in Sec. II. Equations (26) and (28) are used to evaluate both the intrasubband and intersubband transitions due to the confined phonons of Ge-Si and Ge-Ge modes. However, since the Si-Si vibration is unconfined, the calculation of its scattering rate is trivial.[27]

### A. Intrasubband scattering

The intrasubband scattering rate was calculated assuming that the transition originated from the heavy-hole state with a kinetic energy equal to the Si phonon energy to the bottom of the same subband. Therefore, only the process of phonon emission is considered in the calculation. All results are obtained at room temperature. The structure parameters are varied within the limits for producing metastable strained $Si_{1-x}Ge_x$ alloy on the Si substrate.[28] Figure 3 shows the intrasubband transition rates 1-1 within the ground-state heavy-hole subband ($n=1$) due to the Ge-Si and Ge-Ge guided and interface modes as a function of the well width for a $Si_{0.5}Ge_{0.5}$/Si QW. It can be seen that for the intrasubband process the strength of interface mode scattering is about same order of magnitude as that of corresponding guided mode. This is in contrast to the intersubband process discussed later. The scattering rates of both guided and interface modes for Ge-Si and Ge-Ge vibrations increase with the increase of the well width when it is narrow ($L<25$ Å). This

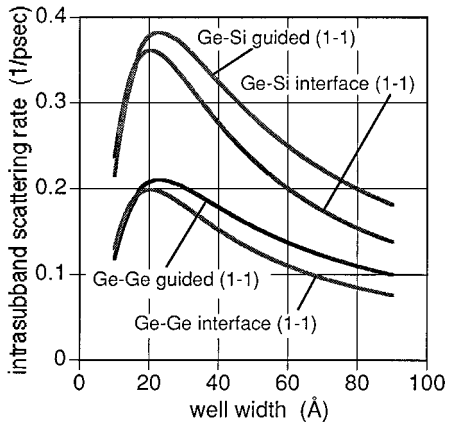


FIG. 3. Intrasubband scattering rates in the lowest subband ($n=1$) due to Ge-Si and Ge-Ge guided and interface modes as a function of well width with $x=0.5$.

is due to the increase of the interference $G$ function with $n=n'=1$ given by Eqs. (24) and (25) as the envelope function for subband 1 becomes more confined in the well region for larger well width. However, the $G$ function increase becomes negligible as the well width increases further since the envelope function has mostly been confined within well region. Examining the interface scattering rate given in Eq. (28), one would expect it to decrease with the further increase of the well width $L$, which is clearly demonstrated in Fig. 3 for both Ge-Si and Ge-Ge phonon interactions. A similar decrease of the interface scattering rate in a GaAs/$Al_xGa_{1-x}$As QW has been reported.[7]

For the guided mode, the scattering rate is given by summing the contributions from the $s$-TO and hybrid of LO and $p$-TO modes. However, the hybrid interaction with the heavy holes is much weaker than the $s$-TO mode, because of the requirements on the hybrid mode to simultaneously satisfy the in-plane momentum conservation and the frequency dispersion Eq. (6). This excludes the interaction of most hybrid modes with the heavy holes, leaving the $s$-TO modes as the dominant scattering mechanism. In fact, the number of allowed $s$-TO vibration modes will increase with the increase of the well width. It is easy to see from Eq. (24) that for the intrasubband process ($n=n'$) the interference $G$ function is nonzero only for even $s$-TO modes ($n_{q_z}=1,3,5\ldots$), and the largest contribution is from the lowest-order mode $n_{q_z}=1$ with higher-order modes being at least two orders of magnitude less. The guided mode scattering for the intrasubband process is therefore practically a single $s$-TO mode interaction and behaves similarly to the interface mode. The difference between the Ge-Si and Ge-Ge vibrations is mainly due to the different weights assigned to them according to the Ge content in the $Si_xGe_{1-x}$ alloy. Our calculation also showed that the 2-2 intrasubband scattering process has very similar behavior as the interface mode scattering and has a slightly higher scattering rate than the guided mode, but overall smaller rates compared to the 1-1 process.

Figure 4(a) shows the total scattering rate as a function of the well width, which is given by summing the contributions from the Ge-Si, Ge-Ge, and Si-Si (unconfined) vibrations. Also shown in Fig. 4(a) is the result calculated neglecting the phonon confinement for comparison. It can be seen that the phonon confinement actually enhances the intrasubband scattering process. However, the opposite is true for the intersubband process to be shown below. Figure 4(b) shows the same result as a function of the Ge content in the alloy for the well width of 40 Å. The difference increases with the increase of the Ge content since the contributions from the confined phonons will increase while that from the unconfined Si-Si vibration decreases.

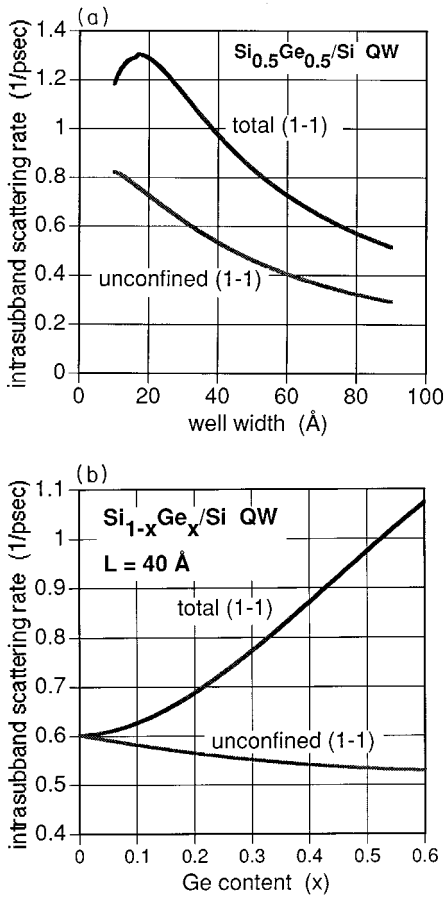


FIG. 4. Total intrasubband scattering rates in the lowest subband ($n=1$) due to Ge-Si, Ge-Ge confined modes, and Si-Si unconfined modes, compared to the bulk intrasubband scattering rate assuming no confinement, (a) as a function of well width with Ge content $x=0.5$ and (b) as a function of $x$ for a well width of 40 Å.

### B. Intersubband scattering

The intersubband scattering rate was calculated assuming that the transition originated from the bottom of a subband $n$ with zero kinetic energy to another subband ($n'\neq n$). Both phonon absorption and emission processes are considered in the calculation. Figure 5(a) shows the 2-1 scattering rate with the Si-Si, Ge-Si, and Ge-Ge components as a function of well width for a $Si_{0.5}Ge_{0.5}$/Si QW. Subband 2 appears at the well width of 20 Å. The total scattering is obtained by summing the contributions derived from the Ge-Si, Ge-Ge, and Si-Si vibrations including both guided and interface modes. But the interface mode scattering is at least two orders of magnitude weaker than the guided mode for the intersubband process. Similar weakness of the interface mode has been shown in a GaAs/$Al_xGa_{1-x}$As QW.[7] The result assuming no confinement is also shown in Fig. 5(a) for comparison. The sharp increase of the scattering rates in the small well width region ($L<25$ Å) is once again due to the increasing confinement in the well region of subband 2, which leads to an increase of the interference $G$ function. Both scattering intensities from Si-Si and unconfined phonons reduce with further increase of the well width. Since initially the narrow well width only allows a small number of guided modes, the guided mode scattering is weak compared to the Si-Si scattering and the total scattering rate follows the dependence of Si-Si vibration. As the number of allowed guided modes increases with increasing well width, the guided mode scattering actually surpasses the Si-Si component, leading to an increase of the total scattering rate. The small discontinuous incremental steps in the Ge-Si, Ge-Ge, and therefore total scattering curves are due to the discrete nature of the increase in the number of allowed guided modes as the well width increases. The sudden drops in the curves occur when the energy separation between the two subbands reduces to less than one of the three phonon energies corresponding to dif-

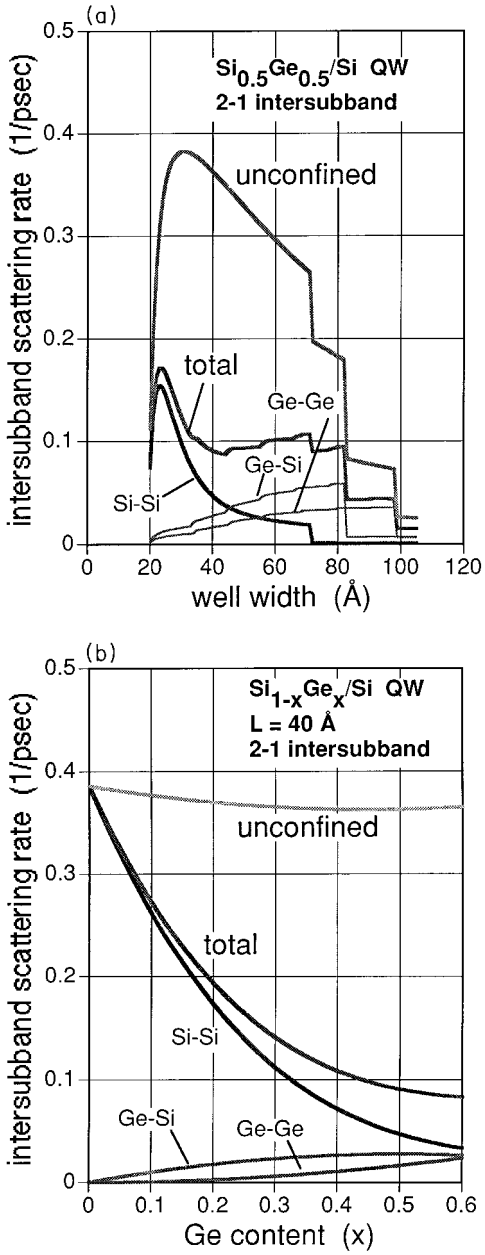


FIG. 5. Total intersubband scattering rates from subband 2 to 1 due to Ge-Si, Ge-Ge confined modes, and Si-Si unconfined modes, compared to the bulk intersubband scattering rate assuming no confinement, (a) as a function of well width with Ge content $x=0.5$ and (b) as a function of $x$ for a well width of 40 Å.

ferent vibrations. Specifically, the drops occurred at $L=72$, 83, and 99 Å corresponding to the Si-Si phonon (64.3 meV), the Ge-Si phonon (50.8 meV), and the Ge-Ge phonon (37.4 meV), respectively. It can be seen in Fig. 5(a) that the phonon confinement reduces the scattering rate by a factor of 2–4 as compared to the case of no confinement. It is therefore important to take into account the phonon confinement effect in estimating the subband lifetimes.

Figure 5(b) shows the 2-1 scattering rates as a function of Ge content in the $Si_{1-x}Ge_x$ alloy for a well thickness of 40 Å. The contributions from the guided modes increases with the Ge content while the unconfined Si-Si component reduces. As a result, the difference between the total scattering rate and the rate obtained assuming no confinement widens with Ge content.

## IV. SUMMARY AND DISCUSSION

In an earlier paper we treated phonon-induced intersubband transitions in $Si_{1-x}Ge_x$/Si MQW structures.[1] The absence of polar optical scattering resulted in subband lifetimes an order of magnitude larger than those in MQW's of III-V semiconductors and without the precipitous decrease at the optical-phonon threshold. This earlier work assumed unconfined, three-dimensional phonons. Noting strong experimental evidence[3] for phonon confinement in $Si_{1-x}Ge_x$/Si MQW's, the present paper extends the earlier treatment to the case in which phonons are confined.

A single $Si_{1-x}Ge_x$ QW with a Si barrier is considered. The decoupled heavy-hole subbands and wave functions are determined by the finite square-well model. Assigning statistical weights to the Si-Si, Ge-Si, and Ge-Ge vibrations in the QW assuming a purely random bond model, the Ge-Si and Ge-Ge modes are treated as confined while the Si-Si modes are extended. The confined modes are of two kinds, guided modes and interface modes. The guided modes consist of the $s$-TO and coupled LO and $p$-TO modes, with the boundary condition that the displacements vanish at the interfaces. In comparison with the guided modes for polar optical phonons, the current choice of basis set that describes the coupling between the $p$-TO and LO modes is neither orthogonal nor complete. Hence the sum rule found for polar LO phonons cannot be applied to the case of nonpolar optical phonons. The interface mode is obtained applying hydrodynamic boundary conditions to the LO and TO modes separately and then requiring that the $z$ component of their sum (not the $x$ component) vanish at the interfaces. The LO mode is a two-dimensional bulk-type solution with constant amplitude in the well and propagating parallel to the interface; the TO mode is an even function (referring to the $z$ component) with a sinusoidal spatial dependence so that the boundary conditions at the interfaces can be satisfied.

The Ge-Ge optical-phonon spectrum in the well region has no overlap with that of Si-Si optical phonons in the barriers, but instead overlaps with that of the acoustic Si phonons. The model for the interface mode derived from the optical-phonon dispersion relations using the hydrodynamic boundary conditions is not without criticism. Further investigation of this subject is underway to provide a more accurate estimate of the intrasubband scattering rates. But we would still expect the intersubband process to be dominated by the guided-mode scattering, which ultimately determines the subband lifetimes.

The intrasubband and intersubband scattering rates are calculated as a function of the QW structure parameters: Ge content $x$ in the $Si_{1-x}Ge_x$ well and the well width $L$. These parameters are varied within the limits reportedly to produce the metastable strained layers of $Si_{1-x}Ge_x$ alloy on Si substrates without introducing a large number of misfit defects. We choose the Ge content of $x=0.5$ as we vary the well

width to give a fair weight of the Ge-Si and Ge-Ge confined modes. We use the fixed well width of 40 Å to allow at least two confined heavy-hole subbands as we vary the Ge content. Our results are as follows. For intrasubband scattering, the scattering by the interface mode is nearly the same as that for the guided mode (Fig. 3) and the total intrasubband scattering with confinement is larger than that without confinement (Fig. 4). However, for intersubband scattering, the interface mode scattering is at least two orders of magnitude smaller than that for the guided mode. Finally, as can be seen from Fig. 5, the total intersubband scattering rate with confinement is a factor of 2–4 smaller than that which would be obtained assuming no confinement. Thus one would expect a factor of 2–4 enhancement in the intersubband lifetimes, which determine population inversion in an intersubband laser.

Finally, we note that the present investigation has considered the scattering of heavy holes whose dispersion is parabolic. The extension to light holes and the split-off band, which are coupled due to spin-orbit coupling and strain[26] and whose dispersions are therefore nonparabolic, would require extension of the theory, but with similar results anticipated.

## ACKNOWLEDGMENTS

The authors wish to thank Dr. Richard A. Soref for discussion and for preparing the figures, Dr. Brian Ridley and Dr. Manuel Cardona for helpful correspondence, and Fen-Yen Chang for assistance in computing. One of the authors (G.S.) wishes to thank the USAF Summer Faculty Research Program for financial support.

[1] G. Sun, L. Friedman, and R. A. Soref, Appl. Phys. Lett. **66**, 3425 (1995).
[2] A. Fasolino, E. Molinari, and J. C. Mann, Phys. Rev. B **39**, 3923 (1989).
[3] S. C. Jain and W. Hayes, Semicond. Sci. Technol. **6**, 547 (1991).
[4] B. K. Ridley, Phys. Rev. B **44**, 9002 (1991).
[5] M. Babiker, J. Phys. C **19**, 683 (1986).
[6] M. Babiker, A. Ghosal, and B. K. Ridley, Superlatt. Microstruct. **5**, 133 (1989).
[7] B. K. Ridley, Phys. Rev. B **39**, 5282 (1989).
[8] M. P. Chamberlain, M. Cardona, and B. K. Ridley, Phys. Rev. B **48**, 14 356 (1993).
[9] B. K. Ridley, Phys. Rev. B **47**, 4592 (1993).
[10] N. C. Constantinou and B. K. Ridley, Phys. Rev. B **49**, 17 065 (1994).
[11] B. K. Ridley, Appl. Phys. Lett. **66**, 3633 (1995).
[12] F. A. Riddoch and B. K. Ridley, Physica B+C **134B**, 342 (1985).
[13] N. Mori and T. Ando, Phys. Rev. B **40**, 6175 (1989).
[14] K. J. Nash, Phys. Rev. B **46**, 7723 (1992).
[15] L. Register, Phys. Rev. B **45**, 8756 (1992).
[16] H. Akera and T. Ando, Phys. Rev. B **40**, 2914 (1989).
[17] A. Fasolino, E. Molinari, and A. Qteish, in *Condensed Systems of Low Dimensionality*, edited by J. L. Beeby *et al.* (Plenum, New York, 1991), p. 495.
[18] H. Rucker, E. Molinari, and P. Lugli, Phys. Rev. B **45**, 6747 (1992).
[19] E. Molinari and A. Fasolino, Appl. Phys. Lett. **54**, 1220 (1989).
[20] E. Molinari, A. Fasolino, and K. Kunc, Superlatt. Microstruct. **2**, 397 (1986).
[21] D. Levi, Shu-Lin Zhang, M. V. Klein, J. Klem, and H. Morkoc, Phys. Rev. B **36**, 8032 (1987).
[22] J. Faist, F. Capasso, D. L. Sivco, A. L. Hutchinson, C. Sirtory, and A. Y. Cho, Science **264**, 553 (1994).
[23] R. A. Soref, Proc. IEEE **81**, 1687 (1993).
[24] B. K. Ridley, *Quantum Processes in Semiconductors* (Clarendon, Oxford, 1982), Chap. 3.
[25] A. Kahan, M. Chi, and L. Friedman, J. Appl. Phys. **75**, 8012 (1994).
[26] G. Sun and L. Friedman, Superlatt. Microstruct. **17**, 245 (1995).
[27] B. K. Ridley, J. Phys. C **15**, 5899 (1982).
[28] J. Bean, Proc. IEEE **80**, 571 (1992).